Electronic Supplementary Material (ESI) for Materials Advances.

SUPPLEMENTARY MATERIAL

Supervalent doping and its effect on the thermal, structural and electrochemical properties of $Li_7La_3Zr_2O_{12}$ solid electrolytes

Janez Košir,[a] Seyedabolfazl Mousavihashemi,[a]‡ Milla Suominen,[a] Anna Kobets,[a] Benjamin P. Wilson,[b] Eeva-Leena Rautama,[a] Tanja Kallio[a]*

[a] Department of Chemistry and Materials Science, School of Chemical Engineering, Aalto University, 02150 Espoo, Finland

[b] Department of Chemical and Metallurgical Engineering, School of Chemical Engineering, Aalto University, 02150 Espoo, Finland

‡ *Current affiliation: VTT Technical Research Centre of Finland, 02150 Espoo, Finland*

1. ICP-OES Measurement

The samples were analyzed in two different sets from two different solutions due to dissolving issues. All the elements were measured using minimum two emission lines to verify the validity of the measurements. For Li, only 460.7 nm was found to be reliable. The recovery-% was 90-99 % except in Al analysis, for which only 83 % was obtained making the Al concentration somewhat unreliable.

Sample preparation and analysis of the dopants, La and Zr: 150 mg of precisely weighted sample was mixed with ca. 3 g lithium metaborate and 150 mg LiBr, melted at 1000 °C for 15 min and immediately poured into 100 ml of HNO_3 (10 %). The cooled and clear solution was diluted and analyzed against a multi-element standard solution. Li analysis could not be carried out from these solutions due to the presence of Li in the used flux mixture.

Li analysis: 30 mg of precisely weighted sample was combined with 10 ml of acid mixture (8 ml conc. HNO_3, 2 ml HBF_4 (50 %)). Each sample was digested in a microwave oven under pressure-assisted vessels (45 mins at 230 °C, gradual heating). Once cooled and diluted, all the samples precipitated partially. Li was measured from these solutions since it is chemically justified to assume the precipitation is Li free under acidic conditions (Li compounds, here particularly LiF, are well-soluble in acids).

The results were studied as experimental (molar) ratios of elements involved. The La:Zr ratio was found to follow the expected stoichiometry surprisingly accurately in all the samples. The experimental amount of each dopant was then proportioned against La.

In the Li analysis, the sample stoichiometry was extracted as a (molar) ratio between the ICP-OES-determined Li and the sample, taking the possible Li deficiency into account in the calculations. Cation ratios, obtained from the dopant-La-Zr analyses, were applied as experimental molar masses in these calculations and full oxygen stoichiometry was assumed.

2. Phase fraction analysis of synthesized LLZO powders

Table S1: Phase fraction composition [wt.%] of doped LLZO powders after synthesis at 950°C.

LLZO - Al	
c-LLZO	23.5 %
t-LLZO	60.3 %
$Li_{0.5}La_2Al_{0.5}O_4$	11.5 %
Li_2ZrO_3	1.9 %
La_2O_3	1.7 %
$LaAlO_3$	1.1 %

LLZO - Ga	
c-LLZO	97.2 %
t-LLZO	0 %
Li_2ZrO_3	1.5 %
La_2O_3	1.3 %

LLZO - Fe	
c-LLZO	17.5 %
t-LLZO	75 %
$LaFeO_3$	2.8 %
$Li_8Fe_5La_{18}O_{39}$	2.4 %
Li_2ZrO_3	2.3 %

LLZO - Ta	
c-LLZO	75 %
t-LLZO	23 %
La_2O_3	2 %

LLZO - Nb	
c-LLZO	67 %
t-LLZO	30.5 %
La_2O_3	2.5 %

LLZO - Sb	
c-LLZO	57 %
t-LLZO	35 %
La_2O_3	5.2 %
Li_7SbO_6	2.8 %

LLZO - W	
c-LLZO	57.5 %
t-LLZO	35 %
La_2O_3	4.8 %
$Li_3W_{0.5}O_3$	2.3 %
ZrO_2	0.4 %

LLZO - Mo	
c-LLZO	37.2 %
t-LLZO	51.8 %
Li_4MoO_5	8.6 %
La_2O_3	2.4 %

3. Morphology of dopant precursor particles

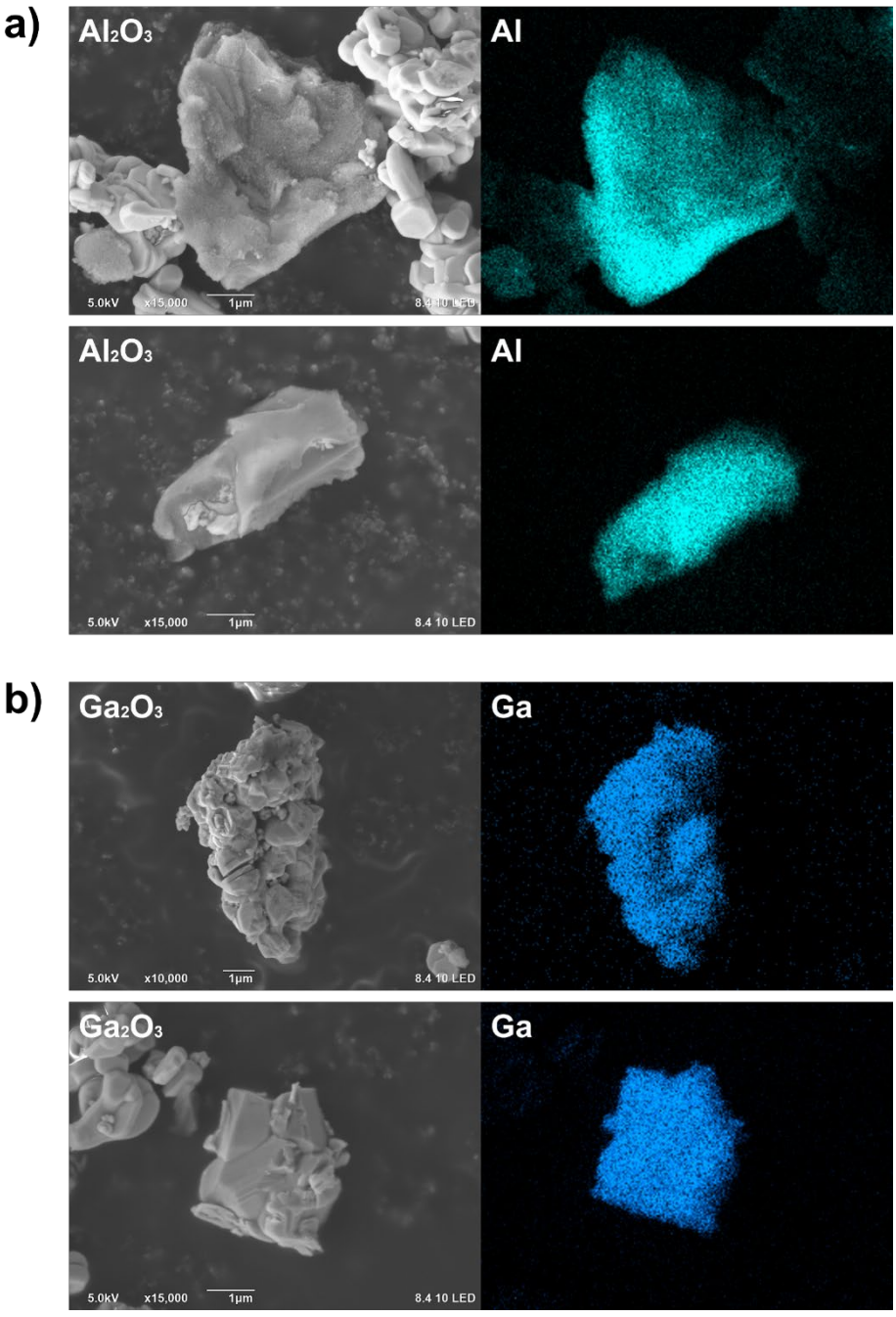

Figure S1: SEM images and corresponding EDS maps showcasing the size and morphology of the dopant precursor particles for a) Al and b) Ga doped LLZO within the LLZO precursor mixture.

4. Rietveld analysis of the sintered samples

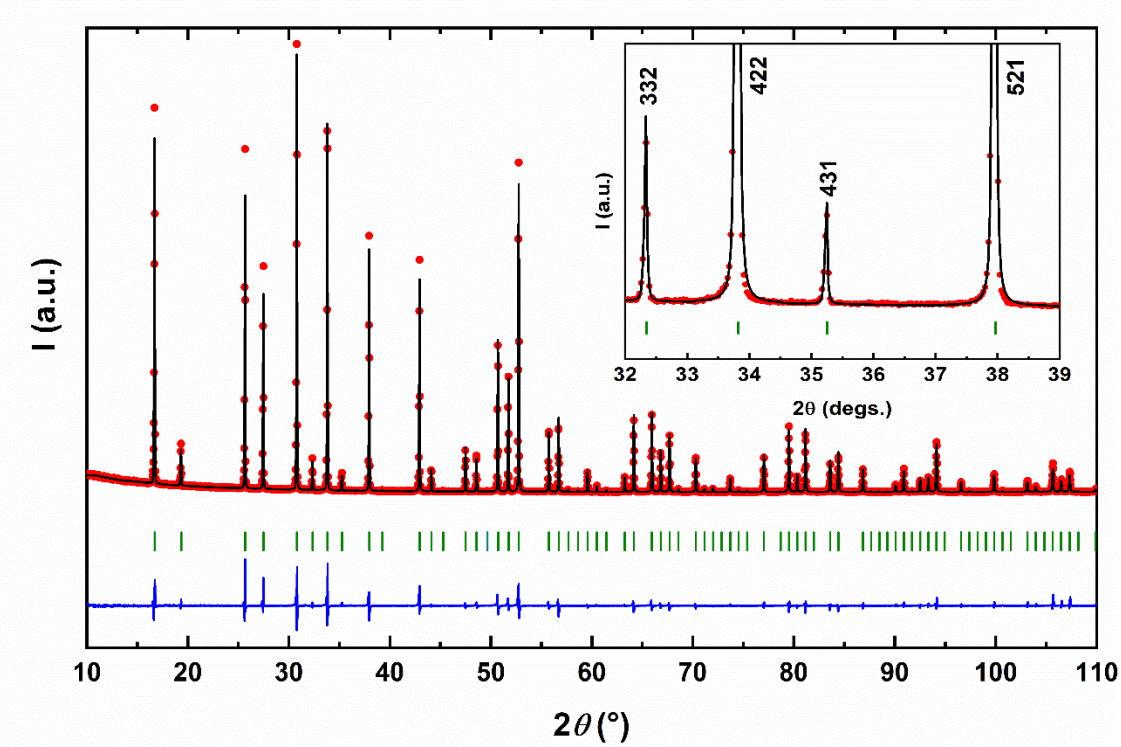

Figure S2: Observed (dots) and calculated (solid) Rietveld refinement profiles of the Al-LLZO sample (space group $Ia\bar{3}d$). The vertical lines indicate the Bragg reflections, and the difference curve is shown at the bottom. The inset emphasizes the peak shape mismatch due to anisotropic right-side broadening in the early *hkl* Bragg peaks (mainly *k* = 2n+1), reflecting their shape throughout the pattern.

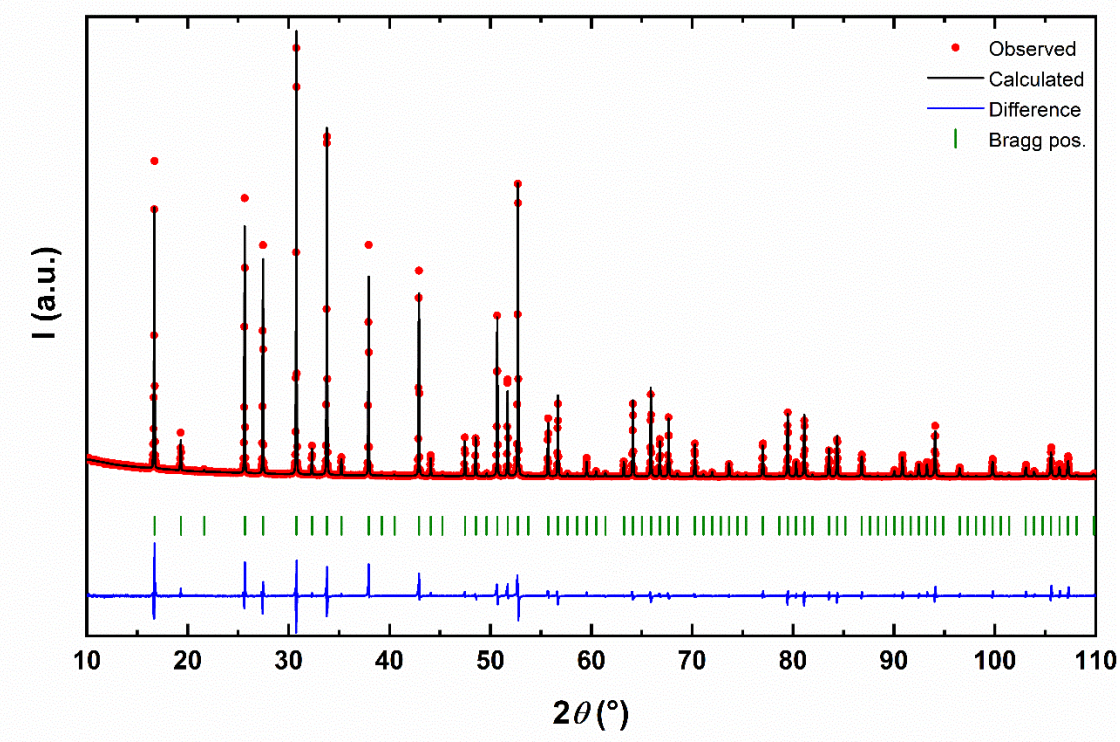

Figure S3: The Rietveld refinement profile of the Ga-LLZO sample (Space Group $I\bar{4}3d$). The crystal symmetry for Ga and Fe samples differ from other samples.

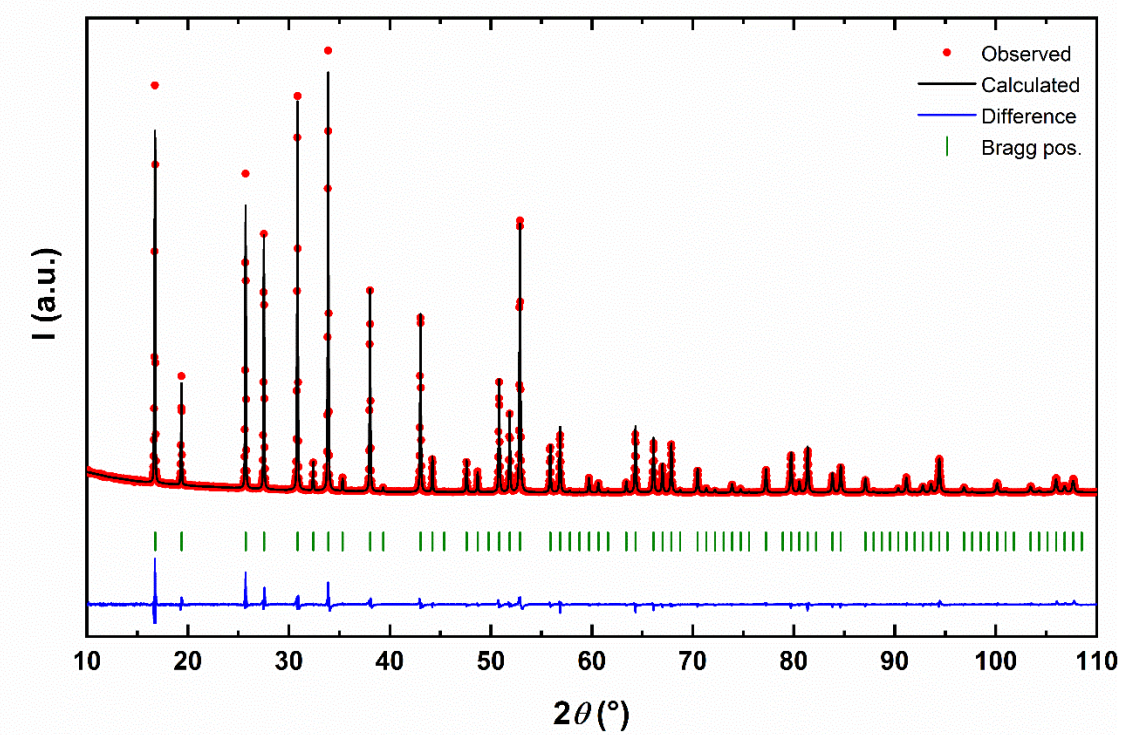

Figure S4: The Rietveld refinement profile of the Ta-LLZO sample (space group $Ia\bar{3}d$). The peak anisotropy effect diminishes towards heavier cations.

5. Raman spectroscopy

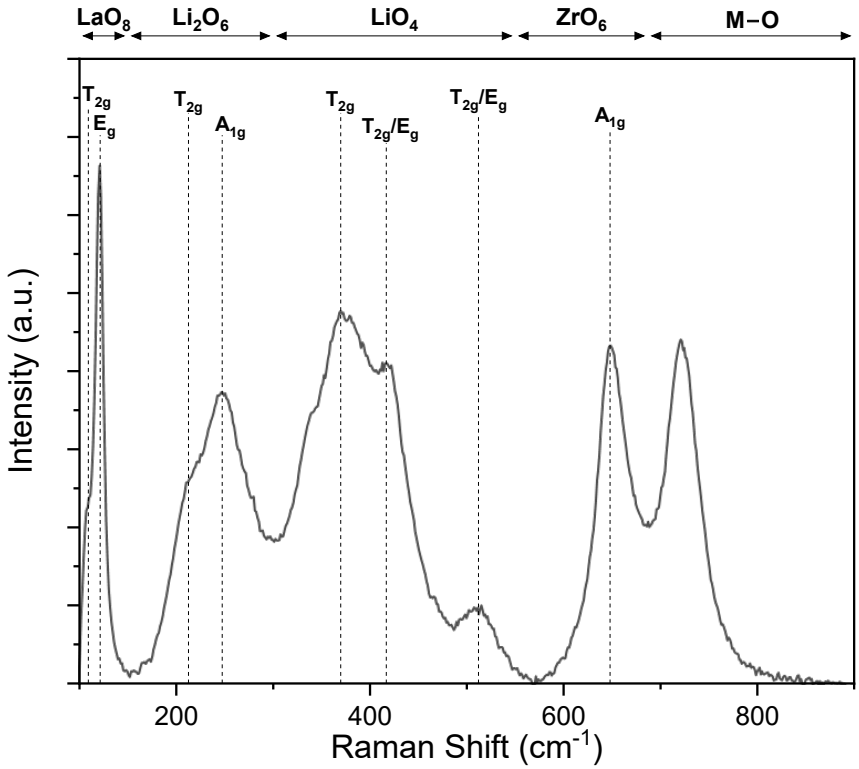

Figure S5: Raman spectrum of Nb-LLZO and the assigned vibrational modes of Raman bands, according to Tietz *et. al.* [1]

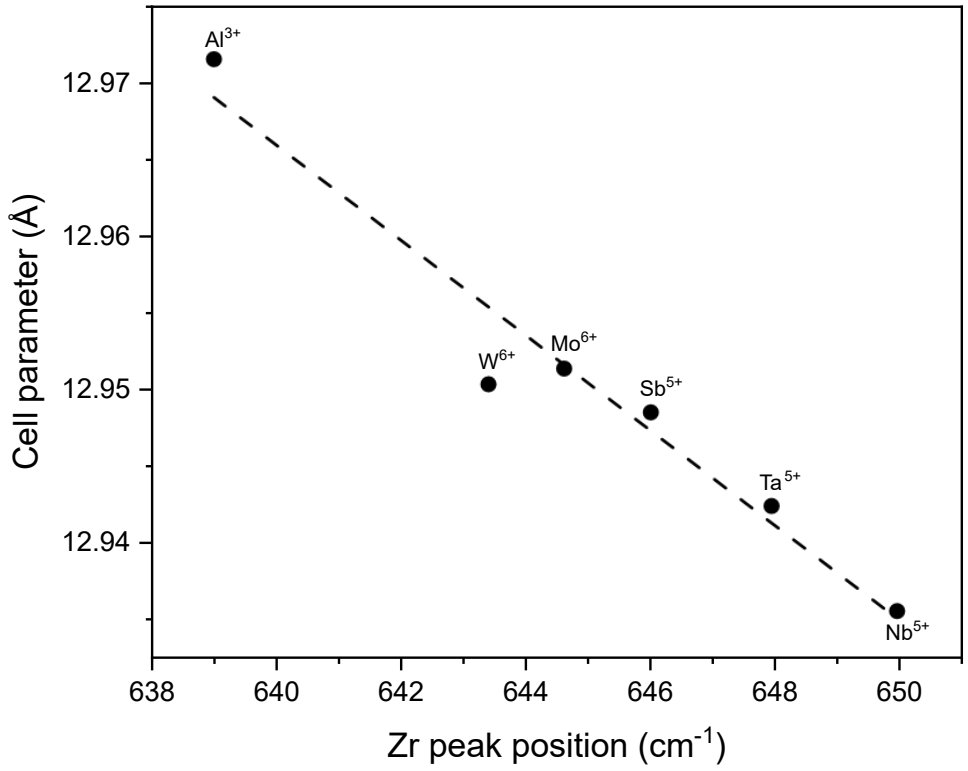

Figure S6: Relationship between the Zr peak position in the Raman spectra of doped LLZO and cell parameter obtained through XRD. Ga and Fe doped LLZO are excluded from this graph due to their disproportionately larger unit cell, caused by a lower symmetry of the crystal structure.

6. Morphology of LLZO pellets

Table S2: Grain shape, size, and fracture type of supervalent doped LLZO samples.

Sample	Grain shape	Average grain size [µm]	Dominant fracture type	Secondary phases
LLZO - Al	Polyhedral	5 - 40	Transgranular and intergranular	$LiAlO_2$ Li_5AlO_4
LLZO - Ga	Spherical	-	Transgranular	-
LLZO - Fe	Polyhedral	5 - 25	Transgranular	$LaFeO_3$
LLZO - Ta	Spherical	5 - 20	Transgranular and intergranular	-
LLZO - Nb	Spherical	3 - 15	Transgranular and intergranular	-
LLZO - Sb	Spherical	5 - 25	Transgranular	-
LLZO - W	Polyhedral	5 - 25	Transgranular and intergranular	-
LLZO - Mo	Spherical/Polyhedral	5 - 50	Transgranular and intergranular	Li_4MoO_5, Li_2MoO_4

7. Electrochemical properties of LLZO pellets

Table S3: Ionic conductivities of doped LLZO samples at elevated temperatures.

	Ionic conductivity (mS/cm)						
	23 °C	**30 °C**	**40 °C**	**50 °C**	**60 °C**	**70 °C**	**80 °C**
LLZO - Al	0.352	0.433	0.617	0.850	1.176	1.553	2.056
LLZO - Ga	1.302	1.593	2.129	2.778	3.559	4.467	5.516
LLZO - Fe	1.115	1.314	1.696	2.161	2.659	3.187	3.745
LLZO - Ta	0.238	0.355	0.556	0.839	1.197	1.614	2.154
LLZO - Nb	0.189	0.266	0.450	0.739	1.154	1.642	2.526
LLZO - Sb	0.315	0.432	0.706	1.123	1.689	2.454	3.378
LLZO - W	0.547	0.793	1.221	1.864	2.664	3.623	4.870
LLZO - Mo	0.303	0.375	0.577	0.866	1.279	1.787	2.358

References

1 F. Tietz, T. Wegener, M. T. Gerhards, M. Giarola and G. Mariotto, *Solid State Ionics*, 2013, **230**, 77–82.